The heavy atom structures and 33S quadrupole coupling constants of 2-thiophenecarboxaldehyde: insights from microwave spectroscopy

Rihab Hakiri, Najoua Derbel, Ha Vinh Lam Nguyen, Halima Mouhib

HAL Id: hal-03182764
https://hal.u-pec.fr/hal-03182764v1

Submitted on 12 Apr 2021

The heavy atom structures and [33]S quadrupole coupling constants of 2-thiophenecarboxaldehyde: Insights from microwave spectroscopy

Rihab Hakiri[a,b], Najoua Derbel[a], William C. Bailey,[c] Ha Vinh Lam Nguyen[d]*, and Halima Mouhib[b]*

[a] *Laboratoire de Spectroscopie Atomique, Moléculaire et Applications, Département de Physique, Faculté des Sciences de Tunis – University of Tunis El Manar, 2092 Manar II, Tunis, Tunisia.*
[b] *Laboratoire Modélisation et Simulation Multi Echelle (MSME), CNRS UMR 8208, Université Paris-Est Marne-la-Vallée, France.*
[c] *(Retired) Chemistry-Physics Department, Kean University, 1000 Morris Avenue, Union, NJ, USA.*
[d] *Laboratoire Interuniversitaire des Systèmes Atmosphériques (LISA), CNRS UMR 7583, Université Paris-Est Créteil, Université de Paris, Institut Pierre Simon Laplace, 61 avenue du Général de Gaulle, 94010 Créteil, France.*

*Corresponding authors:

Halima Mouhib
Laboratoire Modélisation et Simulation Multi Echelle (MSME), CNRS UMR 8208, Université Paris-Est Marne-la-Vallée, France.
Email: halima.mouhib@u-pem.fr

Ha Vinh Lam Nguyen
Laboratoire Interuniversitaire des Systèmes Atmosphériques (LISA), CNRS UMR 7583, Université Paris-Est Créteil, Université de Paris, Institut Pierre Simon Laplace, 61 avenue du Général de Gaulle, 94010 Créteil, France.
Email: lam.nguyen@lisa.u-pec.fr

The heavy atom structures and ^{33}S quadrupole coupling constants of 2-thiophenecarboxaldehyde: Insights from microwave spectroscopy

Abstract

We report on the structures of two conformers of 2-thiophenecarboxaldehyde as obtained using a combination of molecular jet Fourier-transform microwave spectroscopy and quantum chemical calculations. The microwave spectrum was recorded using two spectrometers operating in the frequency ranges of 2.0 GHz to 26.5 GHz and 26.5 GHz to 40.0 GHz. The spectra of all singly-substituted heavy atom isotopologues ^{13}C, ^{18}O, and ^{34}S in their natural abundances could be measured and assigned to determine the experimental gas-phase substitution r_s and semi-empirical r_e^{SE} structures of the most abundant conformer. The spectrum of the ^{33}S isotopologue with its nuclear quadrupole coupling hyperfine structure was analyzed, yielding the complete quadrupole tensor with $\chi_{aa} = -22.63799(76)$, $\chi_- = \chi_{bb} - \chi_{cc} = -18.4892(14)$, and $|\chi_{ab}| = 12.002(33)$ MHz. Quantum chemical calculations for the electric field gradient tensor including corrections with a calibration factor determined from 27 previous studies on the ^{33}S species predicted the ^{33}S nuclear quadrupole coupling constants of 2-thiophencarboxaldehyde with high quality. The experimental results are used to map the observed rotational constants to the corresponding molecular structure obtained from quantum chemical calculations, which predicted two conformers with an energy difference of about 6 kJ·mol^{-1} at the MP2/6-311++G(d,p) level of theory. Insight into the conformational stability of aromatic heterocyclic carboxaldehydes and bond situations of the sulfur atom extracted from the hyperfine structure of the ^{33}S nucleus are discussed within the frame of the current literature. This work provides an important contribution to the study and characterization of sulfur-containing volatile organic compounds.
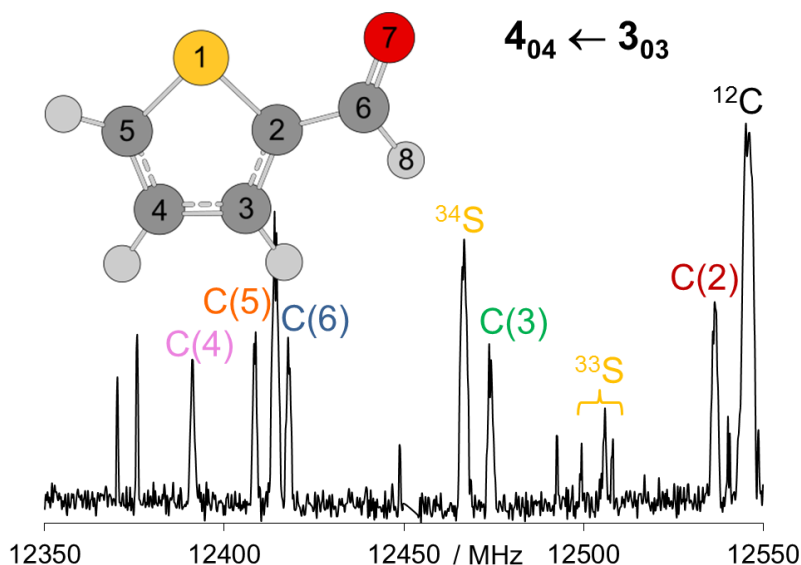
Introduction

2-Thiophenecarboxaldehyde, which will be henceforward referred to as 2TPC, is a chemical compound that belongs to the family of thiophene or thiofurane. These types of small, volatile organic compounds possess numerous applications, e.g., as precursors in the drug and cosmetic industry [1], as agricultural agents [2], and in energetics as fluorescents and organic light-emitting diodes, as well as components in fossil fuels [3-5]. A large number of their alkyl derivatives, e.g., 2-methyltetrahydrofuran-3-one and 2-acetyl-5-methylfural, also contribute to the scent and flavor composition of food, such as coffee beans [6-8] and smoked salmon [9].

In an early investigation, 2TPC has been measured by Mönnig *et al.* in the microwave region from 6 to 20 GHz using a Stark modulated spectrometer, and a small number of low-*J* transitions were reported. The authors assumed an *anti* orientation of the sulfur and the oxygen atom due to steric hindrance [10]. This assumption has been contradicted by the later work of Braathen *et al.*, also using the Stark modulated microwave spectroscopy technique from 12.5 to 40.0 GHz in combination with electron diffraction, Raman, infrared, and matrix isolation spectroscopy, which suggested the *syn* orientation [11]. In the latter work, the microwave spectra were recorded at room temperature and at –40°C, where the vibrational ground state and the three lowest energy vibrationally excited states, v_{27}, v_{19}, and v_{26}, were analyzed, and the spectra of at least five other excited states were visible. To gain insight into the structure of the isolated form of 2TPC, we applied state-of-the-art molecular jet Fourier-transform microwave (MJ-FTMW) spectroscopy in the frequency range from 2.0 to 40.0 GHz [12,13] in combination with quantum

chemical calculations. This joint-venture in experiment and theory is the method of choice to perform reliable conformational sampling of small to medium-sized molecular systems as it allows to identify the lowest energy conformers under jet conditions and to determine the molecular structure with high accuracy [14,15].

In 2TPC, due to conjugation effects with the aromatic ring, the formyl group can only take two possible orientations: *syn* or *anti* with respect to the sulfur atom in the ring. The structure of both conformations of 2TPC is shown in Figure 1. In the case of furfural (denoted as molecule **2** in Figure 1), first studied by Mönnig *et al.* [16,17], the *anti*-conformer was characterized as the most stable structure using microwave measurements, which was later confirmed by Motiyenko *et al*. [18]. For pyrrol-2-carboxaldehyde (2PC) (denoted as molecule **4** in Figure 1) however, the *syn*-conformer was identified as the lowest energy conformer [19]. Due to the contrary results in the literature on the most stable conformation of 2TPC, we were interested in revisiting its microwave spectrum to compare our observed structure of 2TPC with previous results, as well as with the structurally related systems mentioned above. The exchange of oxygen by sulfur in small molecular entities is an interesting phenomenon which often leads to strongly altered physico-chemical properties and hence biological properties. This is well-described for many odorants and flavors where this exchange dramatically alters detection thresholds and olfactory properties [20,21].

The quadrupole hyperfine structure of the ^{33}S nucleus of 2TPC was also studied to extract information on the electric field gradient and the nature of the chemical bonds at the site of the sulfur nucleus. An enormous number of investigations on the hyperfine structures of many nuclei have been reported, e.g. those of ^{14}N [22,23], ^{35}Cl and ^{37}Cl [24], ^{79}Br and ^{81}Br [25], and ^{127}I [26], but only a few of ^{33}S [27], most probably because of the low natural abundance of 0.76% and an expensive preparation (if possible). The high resolution and sensitivity of our experimental setup have enabled the observation of this valuable sulfur species in natural abundance.
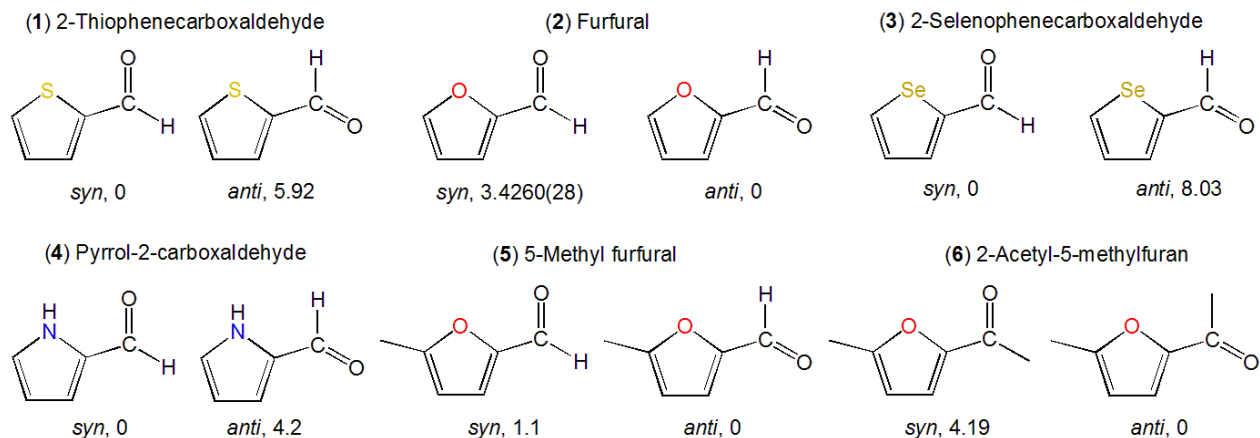
Figure 1. Aromatic five-membered rings with carboxaldehyde substitution at the second ring position and their derivatives: (**1**) 2-Thiophenecarboxaldehyde, (**2**) furfural, (**3**) 2-selenophenecarboxaldehyde, (**4**) pyrrol-2-carboxaldehyde, (**5**) 5-methylfurfural, (**6**) 2-acetyl-5-methylfuran. For each molecule, the two conformers (*syn* and *anti*) with their energy (in kJ·mol^{-1}) relative to the most stable one are given. For all molecules, the molecular symmetry is always C$_s$.

Quantum chemical calculations

Geometry optimizations

Due to the aromatic heterocycle, 2TPC possesses a rigid structure with the formyl group as the only degree of freedom to generate different minima on the potential energy surface. In Figure 2, we show the potential energy curve of 2TPC obtained through rotation of the formyl group in steps of 10° around the dihedral angle $\angle(S_1,C_2,C_6,O_7)$, see Figure 3 for atom labels. This angle was kept at a fixed value while the remaining degrees of freedom were allowed to relax during optimizations at the MP2/6-311++G(d,p) level of theory [28]. We chose this level of theory since previous microwave spectroscopic studies on related sulfur-containing rings such as 2-methyltetrahydrothiophene [29], 2-methyl-1,3-dithiolane [30], and tetrahydrothiophen-3-one [8] have shown that it provides reliable rotational constants that can be used directly for the assignment of the experimental spectra. All calculations were carried out using the *Gaussian 16* program package [31]. The potential energy curve yielded two energy minima, corresponding to a *syn*- and an *anti*-conformer with a dihedral angle 0° and 180°, respectively. These two structures were again optimized at the same level of theory to allow the full structure to relax into the closest local minimum. The nature of the two stationary points was then verified using harmonic frequency

calculations. Both conformers are depicted in Figure 3. Using these structures as starting geometries, new optimizations were carried out with DFT method using the CAM-B3LYP functional [32] with Grimme's dispersion correction [33] and Becke-Johnson damping [34] in combination with the Dunning's basis set aug-cc-pVTZ [35], followed by anharmonic frequency calculations using very tight convergence criteria with an ultrafine grid and including electron mass correction to obtain ground state molecular parameters. The quantum chemical results are summarized in Table 1. The Cartesian coordinates of both conformers are provided in Table S1 in the supplementary material. Using both methods, *syn*-2TPC is predicted as the global minimum structure. The relative energy difference (including the zero-point energy correction) between the two conformers at the MP2 and the B3LYP level is 5.92 kJ·mol^{-1} and 4.79 kJ·mol^{-1}, respectively. In a previous study on carboxaldehydes, Itoh *et al.* studied the energetics of the conformers of 2- and 3-thiophenecarboxaldehydes in argon matrices by means of matrix-isolation infrared spectroscopy [36]. Their analysis using density functional theory and coupled-cluster calculations are in agreement with our results. A study on the kinetics of the isomerization between the two conformers by Pethrick and Wyn-Jones using ultrasonic pulse technique estimated a potential energy barrier of 42 kJ·mol^{-1} [37], which is close to our predicted barrier of interconversion of about 40 kJ·mol^{-1} shown in Figure 2.
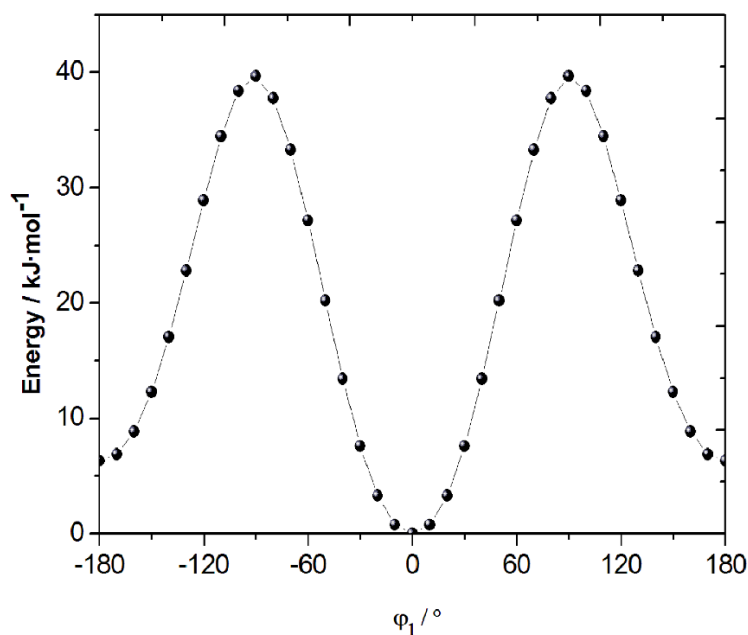

Figure 2. The potential energy curve of 2TPC obtained through rotation of the formyl group by changing the dihedral angle $\angle(S_1,C_2,C_6,O_7)$ in steps of 10° as obtained at the MP2/6-

311++G(d,p) level of theory. Two stable conformers of C_s symmetry are found at 0° (*syn*) and 180° (*anti*), see Figure 1 for the structures. The calculated relative energy difference is 6.4 kJ·mol^{-1}, while the barrier to interconversion of the conformer is approximately 40 kJ·mol^{-1}.
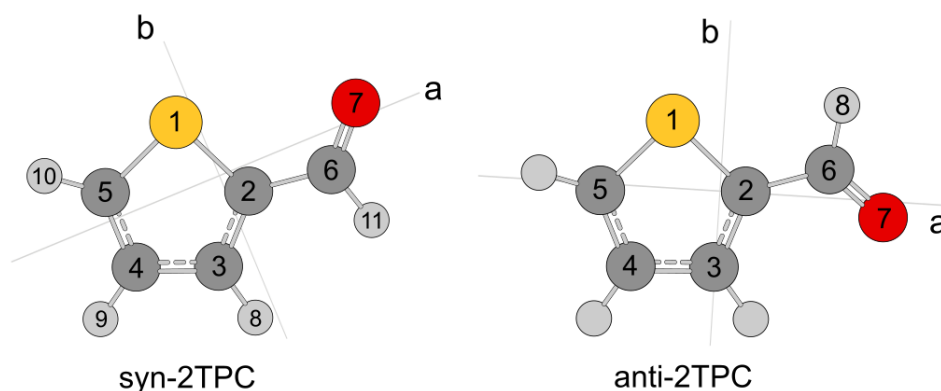

syn-2TPC   anti-2TPC

Figure 3. Molecular structures of the two conformers (*syn* and *anti*) of 2TPC optimized at the MP2/6-311++G(d,p) level of theory (see Table 1) in their principal axes of inertia.

Table 1. Rotational constants A, B, C (in MHz), dipole moment components μ (in Debye), relative electronic energies ΔE (in kJ·mol^{-1}) with respect to the lowest energy conformer, and relative electronic energies including the zero-point energy correction ΔE_{ZPE} (in kJ·mol^{-1}) as obtained at the MP2/6-311++G(d,p) and CAM-B3LYP-D3BJ/aug-cc-pVTZ levels of theory.

| | MP2/6-311++G(d,p) | | B3LYP-D3BJ/aug-cc-pVTZ | |
	syn-2TPC	*anti*-2TPC	*syn*-2TPC	*anti*-2TPC
A_e	5085	5016	5149.9	5098.7
B_e	1876	1784	1898.3	1802.4
C_e	1370	1316	1387.0	1331.7
μ_a	−3.85	−3.77	−3.47	−3.47
μ_b	2.40	−0.46	1.91	−0.36
μ_c	0.00	0.00	0.00	0.00
μ_{total}	4.53	3.80	3.96	3.49
ΔE	0.0	6.37	0.0	4.90
ΔE_{ZPE}	0.0	5.92	0.0	4.79

[33]S Nuclear quadrupole coupling constants

The relation between the components of the nuclear quadrupole coupling tensor, χ_{ij} with those of the electric field gradient tensor, q_{ij} is $\chi_{ij} = (eQ/h) \cdot q_{ij}$. In this equation, h is Planck's constant, Q is the electric quadrupole moment of the nucleus, and e is the fundamental electric charge. Systematic calculations on the quadrupole couplings of the [33]S nucleus were performed using the so-called "basis set method" applied on the MP4 (SDQ) full level of theory [27]. This pure *ab initio* method yielded accurate [33]S nuclear quadrupole coupling constants with deviation of 2 to 3% relative to the largest component and 1% of the whole range of couplings. We prefer a more cost-efficient, semi-empirical method based on the calibration of a particular level of theory, in this case the B3LYP/6-311G(3df,3p) level. The coefficient eQ/h is taken as a best-fit parameter determined by linear regression analysis of calculated q_{ij} on the experimental structures of a number of [33]S molecules versus the corresponding experimental χ_{ij} [38,39], as shown in Figure 4. This calibration procedure permits to correct the systematic errors inherent in calculations at the level of theory in use. The slope of the line illustrated in Figure 4 represents the best-fit parameter eQ/h with the value of $-15.508(43)$ MHz/a.u. For 2TPC, this model was applied on the heavy atom r_s structure of the *syn* conformer determined experimentally with hydrogen structure parameters determined by B3PW91/6-31G(2d,2pd) partial optimization, yielding the quadrupole coupling tensor with the diagonal elements $\chi_{aa} = -22.67$, $\chi_{bb} = 2.44$, and $\chi_{cc} = 20.23$ MHz, as well as the off-diagonal element $\chi_{ab} = 12.02$ MHz. Due to the C_s symmetry of 2TPC, χ_{ac} and χ_{bc} are zero. The standard deviation of the residuals in the calibration is 0.39 MHz, which was taken as the uncertainty in the calculations on NQCCs.
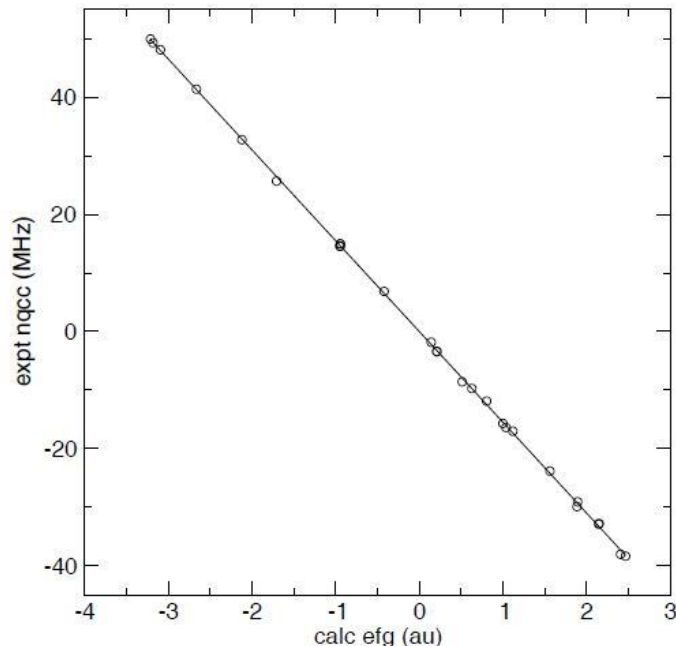
Figure 4. Linear regression of experimental nuclear quadrupole coupling constants, χ_{ii}, versus B3LYP/6-311G(3df,3p) calculated electric field gradients, q_{ii}. The slope, eQ/h, is $-15.508(43)$ MHz/a.u.

Experiment

Measurements

2TPC was purchased from TCI, Eschborn, Germany. To record the microwave spectrum, some drops of the substance were put on a 10 cm length piece of a pipe cleaner. Under a helium stream at a total pressure of 60 - 110 kPa, the mixture 2TPC-helium was expanded through a pulsed nozzle into the cavity. Helium was chosen over argon or neon because of the warmer supersonic jet that enables the observation of high *J* transitions and consequently to obtain accurate centrifugal distortion constants. The microwave spectra were obtained using two MJ-FTMW spectrometers operating in the frequency ranges from 2.0 to 26.5 GHz (the Aachen big cavity) [12] and 26.5 to 40.0 GHz (the Paris small cavity) [13]. At first, we recorded a survey scan from 8.0 to 13.0 GHz, which consists of automatically taken overlapping spectra at a step width of 0.25 MHz with 50 coadded decays for each spectrum. Subsequently, all rotational transitions recorded in the scan were remeasured under high resolution with an instrumental accuracy for isolated lines of approximately 2 kHz. Figure 5 shows part of the broadband scan from 12350 to 12550 MHz, where

the arbitrary intensity is given in a logarithmic scale to increase the weaker signals arising from the ^{33}S and the ^{13}C isotopologues.
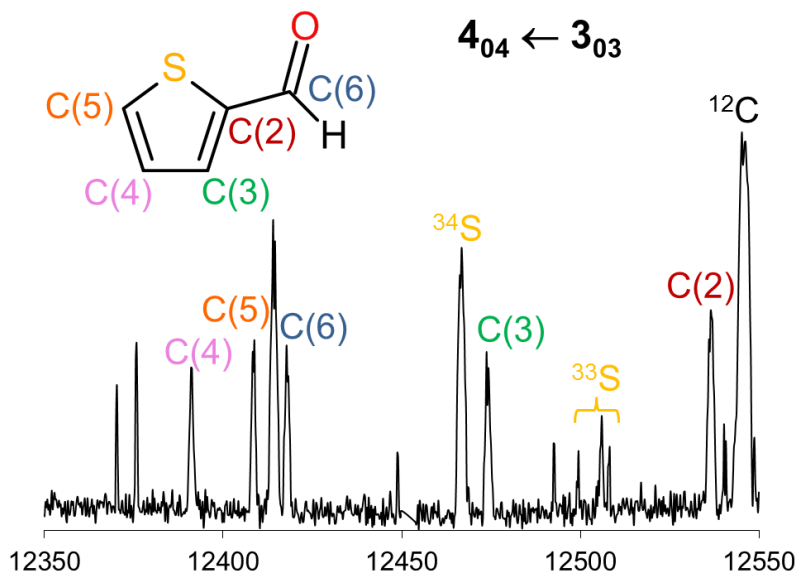

Figure 5. Recorded broadband scan of 2TPC in the frequency range from 12350 to 12550 MHz by overlapping spectra with 50 co-added decays per each spectrum. The intensities are given in arbitrary units. The lines corresponding to the $4_{04} \leftarrow 3_{03}$ transition of the most stable *syn*-conformer are labelled with their corresponding isotopologues and highlighted in color. The color code is provided on the molecular structure at the upper left-hand side of the figure.

Spectral assignment and fits

 The syn-conformer

For the assignment of the spectra, we started with the most stable *syn*-2TPC conformer. The molecular symmetry is C_s; the rotational constants obtained at the MP2/6-311++G(d,p) level of theory are A_e = 5085 MHz, B_e = 1876 MHz, C_e = 1370 MHz, corresponding to a Ray's asymmetry parameter $\kappa = -0.73$ [40], and the dipole moment components are μ_a = 3.85 D and μ_b = 2.40 D. Due to the plane of symmetry, the dipole moment in the *c*-direction is zero. Therefore, we only expect *a*- and *b*-type transitions in the spectrum. With some trial and error, we assigned the first three *a*-type transitions of an *R*-branch, and could easily find more *a*-type line afterwards as described in ref. [41]. Several *b*-type transitions were subsequently assigned and added to the fit. Altogether, 78 *b*-type and 50 *a*-type line of $J \leq 13$ were fitted using the program *SPFIT* [42]. For a

semi-rigid rotor, as in the case of 2TPC, the Hamiltonian only consists of rotational and quartic centrifugal distortion terms using Watson's A reduction and I^r representation. The observed frequency list is given in Table S2 in the supplementary material; the spectroscopic parameters are summarized in Table 2.

In previous studies using the same instruments, e.g. tetrahydrothiophen-3-one [8] and 2-methyltetrahydrothiophene [29], the spectrum of the ^{34}S isotopologue in natural abundance of about 4% could be observed. Since many intense lines remained unassigned in the scan, we were able to assign them to the ^{34}S species of *syn*-2TPC. In total, 81 transitions (24 *a*-type and 57 *b*-type) with $J \leq 10$ and $K_a \leq 5$ were measured and included in the fit. A complete list of ^{34}S transitions is given in Table S3 in the supplementary material. However, after removing all lines belonging to the parent and ^{34}S species, there were still many unassigned lines of weaker intensity in the broadband scan (see for example Figure 3).

After some attempts to assign them to the *anti*-conformer failed, we then suspected that the unassigned lines might belong to the ^{13}C-species of *syn*-2TPC, and could assign all five ^{13}C isotopologues. The rotational constants and all quartic centrifugal distortion constants were determined with high accuracy. They are given in Table 2 along with the parameters of the parent species and the ^{34}S species. To complete the heavy atom structure, we searched for the ^{18}O-isotopologue. The assignment was more difficult because of the low natural abundance of 0.2 %, but was successful by performing small scans around the predicted frequencies with 350 co-added decays instead of 50 decays at each step. Though only 26 lines could be measured, four of five quartic centrifugal distortion constants were fitted with high accuracy (see Table 2). The frequency lists of all ^{13}C- and the ^{18}O-isotopologues are given in Tables S4 and S5 in the supplementary material.

Table 2. Molecular parameters of the parent species, as well as the ^{34}S, ^{13}C, and ^{18}O isotopologues of *syn*-2TPC obtained from the *SPFIT* fits using a semi-rigid rotor approach. Atoms are numbered according to Fig. 1.

Par.[a]	Unit	^{12}C	^{34}S	^{13}C(2)	^{13}C(3)	^{13}C(4)	^{13}C(5)	^{13}C(6)	^{18}O(7)	B3LYP[b]
A_0	MHz	5112.99987(13)	4987.423898(75)	5102.80936(18)	5010.49521(19)	5073.87595(18)	5101.13729(19)	5091.20855(19)	5107.80126(25)	5122.3
B_0	MHz	1887.854961(28)	1886.392598(46)	1887.081327(96)	1885.19324(11)	1862.02128(14)	1862.50335(13)	1865.358355(93)	1796.89608(33)	1888.9
C_0	MHz	1378.741278(19)	1368.664887(32)	1377.590617(83)	1369.765076(72)	1362.106842(84)	1364.326596(71)	1365.144116(67)	1329.23354(21)	1379.9
Δ_J	kHz	0.14961(15)	0.15093(40)	0.1512(13)	0.1477(13)	0.1416(18)	0.1484(18)	0.1486(11)	0.1447(61)	0.1429
Δ_{JK}	kHz	0.8558(16)	0.8693(22)	0.838(11)	0.8584(75)	0.8575(94)	0.7783(92)	0.8182(77)	0.905(23)	0.8189
Δ_K	kHz	0.227(11)	0.1896(28)	0.215(17)	0.161(18)	0.255(29)	0.212(18)	0.256(26)	0.223(27)	0.2192
δ_J	kHz	0.03975(73)	0.0404(20)	0.03908(67)	0.03701(63)	0.03729(84)	0.03952(86)	0.03703(63)	0.0364(32)	0.0380
δ_K	kHz	0.6790(17)	0.6797(54)	0.697(28)	0.724(26)	0.678(32)	0.706(25)	0.671(18)	0.649(89)	0.6448
rms[c]	kHz	1.6	2.1	1.5	1.5	1.7	2.0	1.6	1.8	
N[d]		128	81	49	50	44	45	48	26	

[a] All parameters refer to the principal axis system. Watson's A reduction and I^r representation were used. Standard errors in parentheses are in the units of the last digits.
[b] Calculated values obtained from anharmonic frequency calculations at the CAM-B3LYP-D3BJ/aug-cc-pVTZ level of theory.
[c] Root-mean-square deviation of the fit.
[d] Number of lines.

The ^{33}S isotopologue

To gain insights into the nature of the chemical bonds at the site of the sulfur nucleus, we searched for the ^{33}S isotopologue in natural abundances of 0.75 %. Because the ^{33}S nucleus possesses a nuclear spin $I = 3/2$, hyperfine splittings occur in the microwave spectrum. At the beginning, some small scans of ±10 MHz around the mean values of the frequencies of some ^{32}S (parent species) and ^{34}S transitions with 350 co-added instead of 50 decays at each step were recorded. Figure 6 illustrates a typical survey spectrum of the $2_{12} \leftarrow 1_{01}$ transition of the ^{33}S isotopologue. The calculated values of the nuclear quadrupole coupling constants given in Section *^{33}S Nuclear quadrupole coupling constants* were used to predict the hyperfine structures, which matched well those of the observed spectra. After the fit has been established, further hyperfine components could be measured directly in the high resolution mode. In total, 146 transitions were measured and fitted, yielding the complete quadrupole coupling tensor including the off-diagonal element χ_{ab}. The frequency list of the ^{33}S isotopologue is available in Table S6 in the supplementary material; the spectroscopic parameters are given in Table 3.
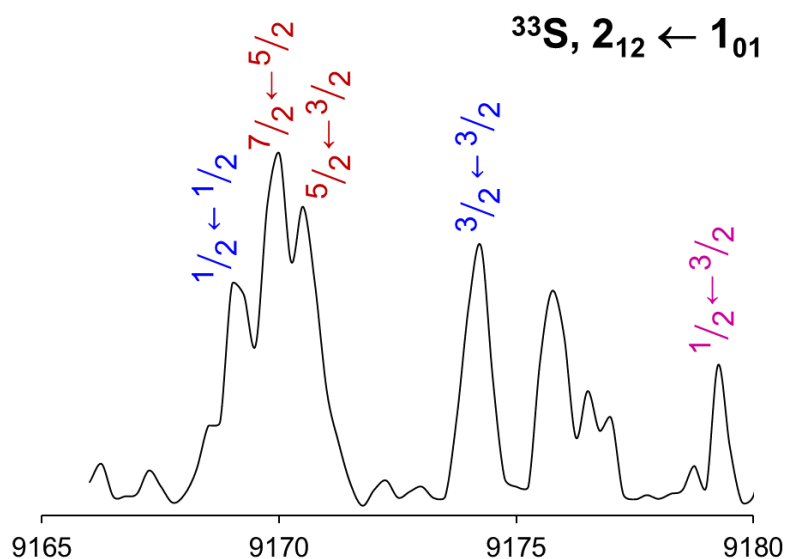

Figure 6. Recorded broadband scan for the $2_{12} \leftarrow 1_{01}$ transition of the ^{33}S isotopologue of *syn-*2TPC in the frequency range from 9166 to 9180 MHz by overlapping spectra with 350 co-added decays per each spectrum. The intensities are given in arbitrary units. The hyperfine transitions are given by F′ ← F.

Table 3. Rotational, centrifugal distortion, and quadrupole coupling constants of the [33]S isotopologue of *syn*-2TPC.

Par.[a]	Unit	[33]S	Calc.
A_0	MHz	5048.74201(16)	5057.3[b]
B_0	MHz	1887.12202(19)	1888.1[b]
C_0	MHz	1373.63197(16)	1374.7[b]
Δ_J	kHz	0.1606(32)	0.1437[b]
Δ_{JK}	kHz	0.820(11)	0.8223[b]
Δ_K	kHz	0.166(25)	0.1997[b]
δ_J	kHz	0.04100(97)	0.0384[b]
δ_K	kHz	0.986(77)	0.6431[b]
χ_{aa}	MHz	−22.63799(76)	−22.67[c]
χ_{bb}[d]	MHz	2.0744(11)	2.45[c]
χ_{cc}[d]	MHz	20.5636(11)	20.23[c]
$\|\chi_{ab}\|$	MHz	12.002(33)	12.02[c]
rms[e]	kHz	2.4	
N[f]		146	

[a] All parameters refer to the principal axis system. Watson's A reduction and I[r] representation were used. Standard errors in parentheses are in the units of the last digits.

[b] Ground state rotational constants obtained from anharmonic frequency calculations at the CAM-B3LYP-D3BJ/aug-cc-pVTZ level of theory.

[c] Obtained from electric field gradient calculations at the B3LYP/6-311G(3df,3p) level of theory on the experimental heavy atom r_s structure with a correction factor $eQ/h = -15.508(43)$ MHz/a.u. (see text).

[d] Derived from the fitted parameters χ_{aa} and $\chi_{bb}-\chi_{cc} = -18.4892(14)$ MHz.

[e] Root-mean-square deviation of the fit.

[f] Number of lines.

The anti-conformer

After the spectra of the parent species, the ^{34}S, ^{13}C, and ^{33}S isotopologues of *syn*-TPC had been assigned and removed from the survey spectrum, some transitions with intensities similar to those of the ^{34}S species of *syn*-TPC still remained. Since the vibrationally excited states ν_{27}, ν_{19}, and ν_{26} reported in Ref. [11] were not visible in our jet-cooled spectrum, where the rotational temperature is very low and only the vibrational ground state is expected, these remaining lines could only arise from the *anti*-conformer. In the broadband scan without transitions of *syn*-2TPC, the characteristic

pattern of the *a*-type *R*-branch $J = 3 \leftarrow 2$ of *anti*-2TPC could be recognized. Finally, 49 *a*-type and 22 *b*-type line of $J \leq 8$ and $K_a \leq 6$ could be assigned and fitted. The observed frequency list is given in Table S7 in the supplementary material; the spectroscopic parameters are shown in Table 4.

Table 4. Molecular parameters of the parent species of *anti*-2TPC obtained from the *SPFIT* fit using a semi-rigid rotor approach.

Par.[a]	Unit	^{12}C	Calc.[b]
A_0	MHz	5048.73045(39)	5070.8
B_0	MHz	1790.808773(90)	1793.0
C_0	MHz	1321.921013(74)	1324.6
Δ_J	kHz	0.08883(97)	0.0855
Δ_{JK}	kHz	0.7775(51)	0.7547
Δ_K	kHz	0.189(83)	0.2581
δ_J	kHz	0.02404(44)	0.0233
δ_K	kHz	0.579(23)	0.5547
rms[c]	kHz	0.5	
N[d]		71	

[a] All parameters refer to the principal axis system. Watson's A reduction and I^r representation were used. Standard errors in parentheses are in the units of the last digits.

[b] Ground state rotational constants obtained from anharmonic frequency calculations at the CAM-B3LYP-D3BJ/aug-cc-pVTZ level of theory.

[c] Root-mean-square deviation of the fit.

[d] Number of lines.

Microwave structure determinations of syn-2TPC

The substitution r_s structure

Using the two programs KRA and EVAL, available at the PROSPE website [43], and the experimental rotational constants of the parent species, the ^{34}S, ^{13}C, and ^{18}O-isotopologues, we determined the microwave structure of *syn*-2TPC with Kraitchman's equation [44]. We used Costain's rule [45] to calculate the uncertainties and the calculated geometry for the sign of the atom coordinates (see Table S1 of the supplementary material). The experimental atom coordinates, as well as the deduced bond lengths and angles are given in Tables 5 and 6. The

experimentally determined r_s structure agrees well with the vibrational averaged structure (r_z) obtained from anharmonic frequency calculations at the CAM-B3LYP-D3BJ/aug-cc-pVTZ level, as visualized in Table 5 and Figure 7.

Table 5. Experimental atom positions of the substitution r_s and the semi-empirical $r_{s\rightarrow e}{}^{SE}$ geometry of *syn*-2TPC obtained with Kraitchman's equations as implemented in the program KRA [43]. Standard errors in parentheses are in the units of the last digits. Atom positions of the equilibrium r_e geometry calculated at the CAM-B3LYP-D3BJ/aug-cc-pVTZ level of theory are also given.

| | r_s geometry | | $r_{s\rightarrow e}{}^{SE}$ geometry | | r_e geometry | | |
	a/Å	b/Å	a/Å	b/Å	a/Å	b/Å	c/Å
S1	0.3239(46)	−1.1275(13)	−0.3269(46)	−1.1259(14)	−0.3400	−1.1303	−0.0001
C2	−0.3313(45)	0.4451(34)	0.3562(42)	0.4497(34)	0.3603	0.4459	0.0000
C3	0.6136(24)	1.4279(11)	−0.6124(25)	1.4239(11)	−0.5993	1.4184	−0.0001
C4	1.92821(78)	0.8851(17)	−1.92323(78)	0.8849(17)	−1.9096	0.8950	0.0001
C5	1.91277(78)	−0.4854(31)	−1.90972(79)	−0.4869(31)	−1.9143	−0.4664	0.0001
C6	−1.79946(83)	0.6582(23)	1.79752(83)	0.6609(23)	1.7988	0.6485	0.0000
O7	−2.62260(57)	−0.2353(64)	2.61885(57)	−0.2330(64)	2.6198	−0.2347	0.0001

Table 6. Experimental r_s and $r_e{}^{SE}$ structural parameters (bond lengths and bond angles) of *syn*-2TPC obtained using the program EVAL (this work) [43] and compared to the values reported by Braathen *et al*. [11]. All *c*-coordinates were set to zero in the EVAL input. Standard errors in parentheses are in the units of the last digits.

| | Bond lengths /Å | | | | Bond angles /° | | |
	r_s	$r_e{}^{SE}$	Ref. [11]		r_s	$r_e{}^{SE}$	Ref. [11]
C2-C3	1.3634(44)	1.3738(43)	1.375(7)	C3-C2-S1	113.51(33)	111.73(31)	111.8(4)
C2-S1	1.7037(42)	1.7173(42)	1.717(4)	S1-C2-C6	120.87(30)	121.78(29)	121.9(10)
C2-C6	1.4836(46)	1.4567(43)	1.466(16)	C2-C3-C4	111.44(20)	112.48(19)	112.2(3)
C3-C4	1.4223(25)	1.4173(25)	1.431(15)	C3-C4-C5	111.79(99)	111.79(10)	112.2(3)
C4-C5	1.3706(36)	1.3718(36)	1.375(7)	C4-C5-S1	112.65(14)	112.55(14)	111.8(4)
C5-S1	1.7138(46)	1.7069(45)	1.717(4)	C2-S1-C5	90.61(21)	91.45(20)	92.0(4)
C6-O7	1.2149(51)	1.2139(51)	1.224(7)	C2-C6-O7	124.39(30)	124.24(30)	123.7(9)
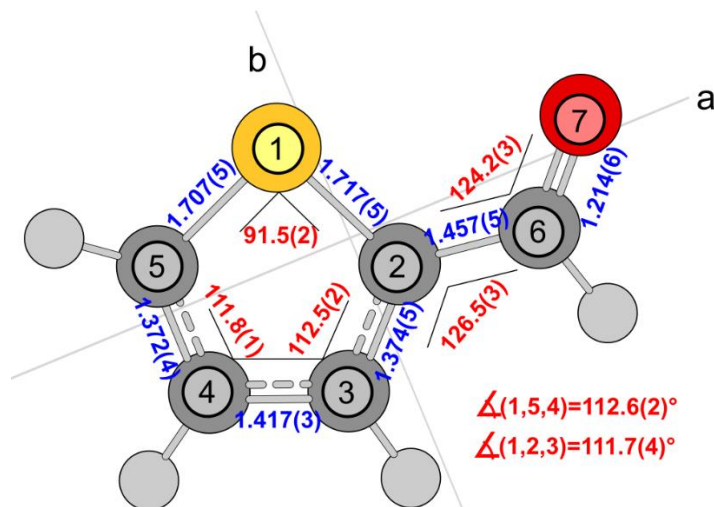
Figure 7. Comparison of the semi-empirical equilibrium $r_{s\to e}^{SE}$ structure of *syn*-2TPC (sulfur in yellow, carbon in gray, oxygen in red) determined by heavy atom substitutions with atom positions of the equilibirum geometry calculated at the CAM-B3LYP-D3BJ/aug-cc-pVTZ level of theory including electron mass correction (smaller circles). The indicated experimental bond lengths (in blue) are given in Å; the experimental bond angles (in red) are in degrees. Standard errors in parentheses are in the unit of the last digit.

The semi-experimental equilibrium r_e^{SE} structures

The substitution r_s structure determination is a method frequently applied in the microwave spectroscopic community, especially if not all singly-substituted heavy atom species are available. The rotational constants deduced from the microwave spectra are input without any correction. Because these constants refer to the vibrational ground state, the r_s structure is not comparable with the equilibrium r_e structure obtained from geometry optimizations. Several alternatives have been proposed to overcome the problems of the r_s structure, one of them is the semi-experimental equilibrium r_e^{SE} structure. Many investigations in the literature have proven that the r_e^{SE} structure is a reasonable choice for structure determination [46-52].

There are two principal methods to determine the r_e^{SE} structure. The first method "corrects" the r_s structure with the differences between the ground state constants $A_{0,calc.}$, $B_{0,calc.}$, $C_{0,calc.}$ and the equilibrium constants A_e, B_e, C_e predicted from anharmonic frequency calculations for the parent species and all isotopologues. The corrected experimental rotational constants $A_{0,exp.}$, $B_{0,exp.}$, and $C_{0,exp.}$ (given in Table S8 in the supplementary material) are subsequently input in the program

KRA [43], yielding the so-called $r_{s \to e}^{SE}$ structure. For *syn*-2TPC where only the heavy atom spectra have been assigned, it is not possible to determine the complete structure due to the lack of information about the hydrogen atom locations. However, hydrogen coordinates from quantum chemical calculations can be taken together with the corrected constants $A_{0,exp.}$, $B_{0,exp.}$, and $C_{0,exp.}$ of all experimentally observed isotopologues to perform a least-squares fit structure using the program STRFIT [53], also available at the PROSPE website [43], resulting in the so-called $r_{0 \to e}^{SE}$ structure. All hydrogen atom locations were allowed to vary in the fitting, but we constrained the bond lengths of three hydrogen atoms attached to the thiophene ring to be the same. The $r_{s \to e}^{SE}$ structure of *syn*-2TPC is also presented in Tables 5 and 6; the $r_{0 \to e}^{SE}$ structure is given in Table S9 in the supplementary material.

Discussion

Molecular geometry

The *syn* and *anti*-conformers of 2TPC were assigned under molecular jet conditions, together with the ^{34}S, ^{33}S, ^{13}C, and ^{18}O-isotopologues of the most stable *syn*-conformer. The spectra of all species were fitted to excellent root-mean-square deviations within the experimental accuracy of 2 kHz. In all fits, the rotation constants and quartic centrifugal distortion constants are well-determined. For the *syn*-conformer, the isotopic shift causes the most changes in the *A* rotational constant of the ^{34}S and ^{13}C(4) isotopologue with differences of 126 MHz and 102 MHz, respectively, comparing to that of the parent species. The *B* and *C* rotational constants remain almost the same in all species, except in the ^{18}O isotopologue, where differences of 91 MHz and 50 MHz are observed for the *B* and the *C* constant, respectively. These values are large if considering the small values of *B* and *C* compared to that of the A constant. The experimental rotation constants of both conformers and all the isotopologues of the *syn*-conformer match well the ground stated constants obtained from anharmonic frequency calculations at the CAM-B3LYP-D3BJ/aug-cc-pVTZ presented in Tables 2 and 3.

The *a*- and *b*- heavy atom coordinates of the r_s and r_e^{SE} structures obtained from isotopic substitutions are determined with high accuracy. The values of the *c*-coordinates are smaller than the errors of the calculations, and therefore were fixed to zero to calculate the bond lengths and bond angles. The bond lengths and bond angles are better determined and agree well, especially

the values of the r_e^{SE} structure, with those derived by Braathen *et al.* by combining complementary spectroscopy methods.

The different bond angle of H_2O (104.5°) compared to H_2S (92.3°) has been discussed as the result from the lower electronegativity of the sulfur atom compared to that of the oxygen atom [54]. The C-S-C angle of 90.61(21)° of 2TPC (see Table 6) is very similar to the value found in hydrogen sulfide. The microwave structure determined for furfural yielded a C-O-C bond angle of 104.7(6)° for the *anti* and 104.8(4)° for the *syn*-conformer [18], which is extremely close to the value found in water and about 14° greater than the C-S-C value of 2TPC. This is also observed for the classical examples of furan (106.56(2)° [55]) and thiophene (92.10(6)° [56]) with a difference in angle of 14.46(8)°. Though the microwave r_s structure could not be determined in 2,5-dimethylfuran [57] and 2,5-dimethylthiophene [58], the angle between the methyl group axes and the principal *a*-axis determined by methyl internal rotation yielded information on the difference between the C-O-C and C-S-C angles due to the C_{2v} symmetry of the molecules. This is 27.2840(85)° for the former [57] and 14.5931(78)° for the latter [58], leading to a difference of 12.7°, which shows that the C-O-C angle in 2,5-dimethylfuran is larger than the C-S-C angle in 2,5-dimethylthiophene (see also ref. [57] for more details).

Conformational stability

From the observed relative intensity, the experimental spectrum of *syn*-2TPC strongly dominates that of *anti*-2TPC, which is about at the level of the [34]S species of *syn*-2TPC in natural abundance of 4%. Quantitative statement on the conformational intensity and stability is not attempted due to the lack of dipole moment measurements and the trust in intensity ratio of the current setup. A chirped pulse spectrum [59] of 2TPC would be needed to obtain more reliable intensity for quantitative comparison.

As mentioned in the introduction, the gas-phase microwave structures of two other aromatic five-membered rings related to 2TPC (**1**), namely furfural (**2**) [16-18] and 2PC (pyrrole-2-carboxaldhyde) (**4**) [19], have been reported in the literature (for molecule numbering see Figure 1 and 8). The molecular geometries are very similar and exhibit two stable conformers featuring the formyl group in *anti* or *syn* position, but the heteroatom in the ring has a significant effect on the conformational stability. The oxygen analogue of 2TPC (**1**), furfural (**2**), has been studied in the microwave region from 7 to 26 GHz [16,17] and subsequently in the millimeter wave and terahertz range from 49 to 330 GHz [18]. The microwave structures of both, *syn* and *anti*-furfural,

were reported and the *anti*-conformer is by 3.4260(28) kJ·mol^{-1} lower in energy than the *syn*-conformer [60]. This is opposite to the observations found for 2TPC (**1**), where the *syn*-conformer is the most stable, as well as in 2PC (**4**), where the energy of the *anti*-form is estimated to be at least 1 kcal·mol^{-1} (4.2 kJ·mol^{-1}) higher than the *syn*-form [19].

The stability of a conformer may result from the interaction between the aromatic ring and the formyl group, as well as conjugation effects. However, these two effects may explain the favorable planar forms due to a maximum overlap between the π-orbitals (confirmed by the value of the inertial defect very close to zero: −0.008 uÅ^2) but not the preference of the *syn*-form over the *anti*-conformation. A reason for the latter may be the dipole-dipole interaction, as illustrated in Figure 8. The dipole moment of the aromatic ring is directed along the bisector of the C-X-C angle (X = O,S,N). In the case of 2PC (**4**), the dipole moment of 1.74(2) D of the pyrrole ring [61] is along the direction of the lone-pair electrons towards the nitrogen atom. In the *syn*-conformer, it conjoins with the dipole moment of the aldehyde group (2.33 D in formaldehyde [62]), pointing from the oxygen atom towards the carbon atom and stabilize this form, while in the *anti*-conformer, the dipoles repel each other. In both molecules, furfural (**2**) and 2TPC (**1**), the dipole moment of 0.661(6) D and 0.55(1) D of the furan [63] and the thiophene ring [64], respectively, directs from the ring center towards the heteroatom and repels the dipole moment of the aldehyde group in the *syn* conformation.
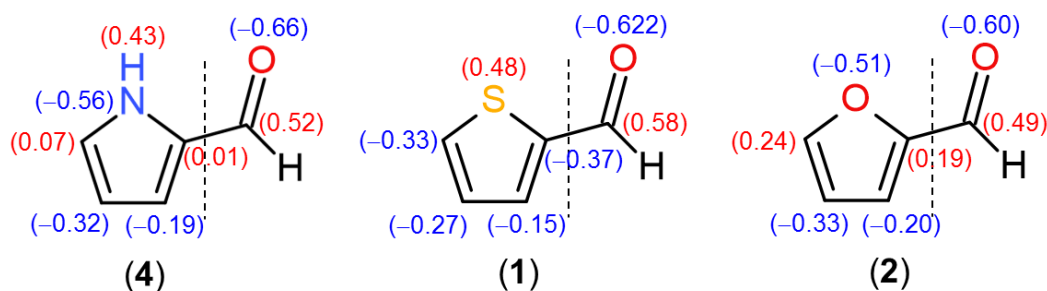

Figure 8. From left to right: pyrrole-2-carboxaldehyde (**4**), 2-thiophenecarboxaldhyde (**1**, this work), and furfural (**2**). The dotted line divides each molecule into two parts: the formyl group and the aromatic heterocycle. The charges of all heavy atoms and the hydrogen atom attached to the nitrogen atom in (**4**) obtained from NBO calculations are indicated in parentheses.

The dipole-dipole interaction may account for the destabilization of the *syn*-form in furfural (**2**), but not in 2TPC (**1**), where the *syn*-form remains more stable. Theoretical work on 2-

selenophenecarboxaldehyde (2SeC) (**3**) predicted that in the selenium analogue, the *syn*-conformer is about 8 kJ·mol^{-1} lower in energy than the *anti*-form [65]. Obviously, changing oxygen by sulfur or selenium reverses the conformational stability of 2-carboxaldehyde. It is widely discussed that the higher stability of the *syn*-form in 2TPC (**1**) and 2SeC (**3**), which is in addition destabilized by orbital interactions, is mainly due to electrostatic interaction between the oxygen atom of the carbonyl group and the sulfur or the selenium atom in the ring [66]. The negative charges on the oxygen atoms of furfural (**2**) stabilizes the *anti*-conformer, while the *syn*-form is favored by the opposite charges on oxygen and sulfur or selenium atoms in 2TPC (**1**) and 2SeC (**4**) [67], as visualized also in Figure 8 with the charge data obtained from NBO calculations. A further example to support this argument is the stability of the *anti*-form in two furfural derivatives, methyl furfural (**5**) [68] and 2-acetyl-5-methylfuran (**6**) [69], where the *anti*-conformer (called *cis* in ref. [68]) is also 1.1 kJ·mol^{-1} and 4.19 kJ·mol^{-1}, respectively, lower in energy than the *syn* conformer (called *trans* in ref. [68]). We note that in the case of methyl furfural (**5**), a methyl substitution (electron donor group) in the 5-position of the ring decreases the energy difference between the two conformers from about 3.4 kJ·mol^{-1} in the case of furfural (**2**) [60] to 1.1 kJ·mol^{-1} [68].

The ^{33}S χ_{cc} constant

The χ_{cc} quadrupole coupling constant of the ^{33}S nucleus of *syn*-2TPC can be compared directly with that of other molecules with C$_s$ symmetry, because the principal *c*-axis is perpendicular to the molecular plane and collinear with one principal axis of the coupling tensor. From the value of χ_{cc} found for all molecules given in Figure 8, we note three distinct groups. The first group contains aromatic five-membered rings, where the values of χ_{cc} in 2TPC (**1**) and thiophene (**2**) [70] are very similar (for molecule numbering see Figure 8). Despite the well-known $-$I effect of the aldehyde group, the ^{33}S field gradient tensor remains essentially the same, indicating that the effect of carboxylation is of minor importance. If a nitrogen atom is present in the ring, the χ_{cc} value changes, but stays around the value of 21 MHz of thiophene (**2**). In the case of thiazole (**3**), where the nitrogen atom is located at the third position of the ring and the sulfur bonding situation is still C−S−C, the χ_{cc} value decreases comparing to that of thiophene (**2**) to about 19 MHz [71]. If the bonding situation changes to N−S−C, as in the case of isothiazole (**4**), the χ_{cc} value increases to 24.27(1) MHz [72].

The second group consists of molecules with the bonding situation C−S−C of sulfur, but they do not contain a π-conjugated system. The χ_{cc} values of 48.14(1), 47.69(1), and 49.3451(14) MHz found for dimethylsulfide (**6**) [73], isothiocyanatomethane (**7**) [74], and thiirane (**8**) [27], respectively, are very similar. By comparing the C−S−C angle of these three molecules, which are 98.5° [75], 99.2° [76], and 48.2° [77], respectively, it is possible that the smaller the angle is, the larger χ_{cc} becomes. However, there are not enough data points to support this statement. And if this is true, structural changes obviously only has minor impact on χ_{cc}, i.e. a decrease of 51.0° in the angle between (**7**) and (**8**) leads to an increase of about 1.7 MHz in χ_{cc}. A special case of this group is H₂S, where the sulfur atom is bond to two hydrogen atoms and the value of χ_{cc} is only 41.42(6) MHz [78].

The sulfur atom of the two molecules in the third group, dimethylsulfoxide (**9**) and thioformaldehyde (**10**), forms a double bond to a/the neighbouring atom, though the bonding situation is quite different in (**9**) and (**10**). In dimethylsulfoxide (**9**), sulfur plays the positive pole in the bond, but in thioformaldehyde (**10**), the partial charge on the sulfur atom is negative. Therefore, the value of χ_{cc} in dimethylsulfoxide (**9**) [79] has a different sign than in thioformaldehyde (**10**) [80]. The value of approximately 35 MHz of χ_{cc} (without considering its sign) found dimethylsulfoxide (**9**) [79] and thioformaldehyde (**10**) [80] differs from that of about 21 MHz of the five-membered ring group [70-72] and that of about 48 MHz of the C−S−C group [27,73,74]. Further studies on the ³³S isotopologues are needed to verify and expand this classification.
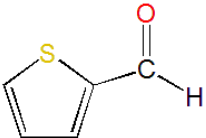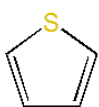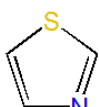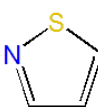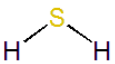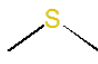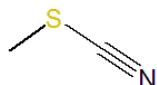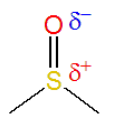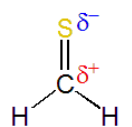

Figure 9. Comparison of the ³³S quadrupole coupling constant χ_{cc} of *syn*-2TPC with a selection of molecules featuring C$_s$ symmetry. Group 1: (**1**) 2-Thiophenecarboxaldehyde (this work), (**2**)

thiophene [70], (**3**) thiazole [71], and (**4**) isothiazole [72]. Group 2: (**5**) Hydrogen sulfide (special case) [78], (**6**) dimethyl sulfide [73], (**7**) isothiocyanatomethane [74], and (**8**) thiirane [27]. Group 3: (**9**) Dimethylsulfoxide [79] and (**10**) thioformaldehyde [80].

Conclusion

Using a combination of high resolution microwave spectroscopy and quantum chemical calculations, we identified the two conformers of 2TPC and the ^{34}S, ^{33}S, ^{13}C, and ^{18}O-isotopologues of the most stable *syn*-conformer under molecular jet conditions. This allowed us to determine with high accuracy the heavy atom microwave substitution r_s and semi-experimental r_e^{SE} structures of *syn*-2TPC. The spectrum of *syn*-2TPC clearly dominates that of *anti*-2TPC, revealing that in five-membered rings, the *syn* conformation is energetically more favorable than the *anti* conformation if a sulfur atom is present in the aromatic ring. Through comparison with related aromatic heterocycles, an explanation based on dipole-dipole interactions is proposed which may account for the stabilizing effects dominating in the most abundant structures. Our work nicely completes the available studies on 2TPC reported in the literature, which is important to improve our understanding on the structures of sulfur containing volatile organic compounds and of five-membered rings in general. The χ_{cc} element of the ^{33}S nuclear quadrupole coupling tensor was compared with that of other molecules with C_s symmetry, making a connection between this important parameter with the nature of the sulfur bonds. This work aligns well with previous reports on volatile organic compounds, where high resolution microwave spectroscopy allowed to elucidate the gas-phase structure of the isolated species without any influence from the environment such as solvent or crystal field effects. For future studies, it will be interesting to use this knowledge for directed structural comparisons of these species in the condensed phase. Here, microwave spectroscopy under molecular jet conditions may again be able to provide crucial insight on the formation of stable water complexes in the gas-phase that can be interpreted as the first step to micro-solvation of these molecules before studying them in the bulk or in the solid phase.

Disclosure statement

No potential conflict of interest was reported by the authors.

References

[1] A.C. Razus, L. Birzan, V. Tecuceanu, M. Cristea and C. Enache, Arkivoc **11**, 210 (2008).

[2] P. Caboni, G. Sarais, N. Aissani, G. Tocco, N. Sasanelli, B. Liori, A. Carta and A. Angioni, J. Agric. Food Chem. **60**, 7345 (2012).

[3] S. Kumar, P.K. Dutta and P. Sen, Carbohydr. Polym. **80**, 563 (2010).

[4] H. Li, X. Chen, J. Wu, Y. Zhang, X. Liu, Q. Shi, S. Zhao, C. Xu and C. S. Hsu, Energ. Fuel. **33**, 1797 (2019).

[5] C. Zhang, L. Huang, Q. Tang, Y. Xu, X. Lan, J. Li, W. Liu and H. Zhao, Energ. Fuel. **32**, 12495 (2018).

[6] M.A. Gianturco, A.S. Giammarino, P. Friedel and V. Flanagan, Tetrahedron **20**, 2951 (1964).

[7] N. Yang, C. Liu, X. Liu, T.K. Degn, M. Munchow and I. Fisk, Food Chem. **211**, 206 (2016).

[8] H. Mouhib, V. Van and W. Stahl, J. Phys. Chem. A **117**, 6652 (2013).

[9] V. Varlet, C. Knockaert, C. Prost and T. Serot, J. Agric. Food Chem. **54**, 3391(2006).

[10] F. Mönnig, H. Dreizler and H.D. Rudolph, Z. Naturforsch. **20a**, 1323 (1965).

[11] G.O. Braathen, K. Kveseth and C.J. Nielsen, J. Mol. Struct. **145**, 45 (1986).

[12] J.-U. Grabow, W. Stahl and H. Dreizler, Rev. Sci. Instrum. **67**, 4072 (1996).

[13] I. Merke, W. Stahl and H. Dreizler, Z. Naturforsch. **49a**, 490 (1994).

[14] E.J. Cocinero, A. Lesarri, P. Écija, F.J. Basterretxea, J.-U. Grabow, J.A. Fernández, and F. Castaño, Angew. Chemie Int. Ed. **51**, 3119 (2012).

[15] D. Loru, M.M. Quesada-Moreno, J.R. Avilés-Moreno, N. Jarman, T.R. Huet, J.J. López-González and M.E. Sanz, ChemPhysChem **18**, (2017).

[16] F. Mönnig, H. Dreizler and H.D. Rudolph, Z. Naturforsch. **20a**, 1323 (1965).

[17] F. Mönnig, H. Dreizler and H.D. Rudolph, Z. Naturforsch. **21a**, 1633 (1966).

[18] R.A. Motiyenko, E.A. Alekseev, S.F. Dyubko and F.J. Lovas, J. Mol. Spectrosc. **240**, 93 (2006).

[19] K.M. Marstokk and H. Møllendal, J. Mol. Struct. **23**, 93 (1974).

[20] A. Goeke, Sulfur Reports **23**, 243 (2002).

[21] R. Zhang, Y. Pan, L. Ahmed, E. Block, Y. Zhang, V.S. Batista and H. Zhuang, Chem. Senses **43**, 357 (2018).

[22] R. Kannengießer, W. Stahl and H.V.L. Nguyen, J. Phys. Chem. A **120**, 5979 (2016).

[23] J.B. Graneek, W.C. Bailey and M. Schnell, Phys. Chem. Chem. Phys. **20**, 22210 (2018).

[24] K.R. Nair, S. Herbers, A. Lesarri and J.-U. Grabow, J. Mol. Spectrosc. **361**, 1 (2019).

[25] F.E. Marshall, N. Moon, T.D. Persinger, D.J. Gillcrist, N.E. Shreve, W.C. Bailey and G.S. Grubbs II, Mol. Phys. **117**, 1351 (2019).

[26] E.A. Arsenault, D.A. Obenchain, W. Orellana and S.E. Novick, J. Mol. Spectrosc. **338**, 72 (2017).

[27] B. Kirchner, H. Huber, G. Steinebrunner, H. Dreizler, J.-U. Grabow and I. Merke, Z. Naturforsch. **52a**, 297 (1997).

[28] C. Møller and M. S. Plesset, Phys. Rev. **46**, 618 (1934).

[29] V. Van, C. Dindic, H.V.L. Nguyen and W. Stahl, ChemPhysChem **16**, 291 (2015).

[30] V. Van, W. Stahl, M. Schwell and H.V.L. Nguyen, J. Mol. Struct. **1156**, 348 (2018).

[31] M.J. Frisch, G.W. Trucks, H.B. Schlegel, G.E. Scuseria, M.A. Robb, J.R. Cheeseman, G. Scalmani, V. Barone, G.A. Petersson, H. Nakatsuji, X. Li, M. Caricato, A.V. Marenich, J. Bloino, B. G. Janesko, R. Gomperts, B. Mennucci, H.P. Hratchian, J.V. Ortiz, A.F. Izmaylov, J.L. Sonnenberg, D. Williams-Young, F. Ding, F. Lipparini, F. Egidi, J. Goings, B. Peng, A. Petrone, T. Henderson, D. Ranasinghe, V.G. Zakrzewski, J. Gao, N. Rega, G. Zheng, W. Liang, M. Hada, M. Ehara, K. Toyota, R. Fukuda, J. Hasegawa, M. Ishida, T. Nakajima, Y. Honda, O. Kitao, H. Nakai, T. Vreven, K. Throssell, J.A. Montgomery, Jr., J. E. Peralta, F. Ogliaro, M.J. Bearpark, J.J. Heyd, E.N. Brothers, K.N. Kudin, V.N. Staroverov, T.A. Keith, R. Kobayashi, J. Normand, K. Raghavachari, A.P. Rendell, J.C. Burant, S.S. Iyengar, J. Tomasi, M. Cossi, J.M.

Millam, M. Klene, C. Adamo, R. Cammi, J.W. Ochterski, R.L. Martin, K. Morokuma, O. Farkas, J.B. Foresman and D.J. Fox, Gaussian 16, Revision B.01, Inc., Wallingford CT, 2016.

[32] W. Kohn, A.D. Becke and R.G. Parr, J. Phys. Chem. **100**, 12974 (1996).

[33] S. Grimme, J. Antony, S. Ehrlich and H. Krieg, J. Chem. Phys. **132**, 154104 (2010).

[34] S. Grimme, S. Ehrlich and L. Goerig, J. Comp. Chem. **32**, 1456 (2011).

[35] T.H. Dunning Jr., J. Chem. Phys. **90**, 1007 (1989).

[36] T. Itoh, N. Tanaka, H. Nishikiori and T. Fujii, Chem. Phys. Lett. **514**, 247 (2011).

[37] R.A. Pethrick and E. Wyn-Jones, *J. Chem. Soc. A* 713 (1969).

[38] W.C. Bailey, J. Mol. Spectrosc. **209**, 57 (2001).

[39] W.C. Bailey, Calculation of Nuclear Quadrupole Coupling Constants in Gaseous State Molecules. <http://nqcc.wcbailey.net/index.html>.

[40] B.S. Ray, Zeitschrift Für Phys. **78**, 74 (1932).

[41] H. Mouhib, J. Phys. B: At. Mol. Opt. Phys. **47**, 143001 (2014).

[42] H.M. Pickett, J. Mol. Spectrosc. **148**, 371 (1991).

[43] Z. Kisiel, PROSPE-Programs for ROtational SPEctroscopy, available at http://info.ifpan.edu.pl/~kisiel/prospe.htm.

[44] J. Kraitchman, Am. J. Phys. **21**, 17 (1953).

[45] C.C. Costain, Trans. Am. Crystallogr. Assoc. **2**, 157 (1966).

[46] J. Demaison, M.K. Jahn, E.J. Cocinero, A. Lesarri, J.-U. Grabow, J.-C. Guillemin and H.D. Rudolph, J. Phys. Chem. A **117**, 2278 (2013).

[47] B.J. Esselman, B.K. Amberger, J.D. Shutter, M.A. Daane, J.F. Stanton, R.C. Woods and R.J. McMahon, J. Chem. Phys. **139**, 224304 (2013).

[48] S. Herbers, P. Kraus and J.-U. Grabow, J. Chem. Phys. **150**, 144308 (2019).

[49] F. Pawłowski, P. Jørgensen, J. Olsen, F. Hegelund, T. Helgaker, J. Gauss, K.L. Bak and J.F. Stanton, J. Chem. Phys. **116**, 6482 (2002).

[50] E. Penocchio, M. Mendolicchio, N. Tasinato and V. Barone, Can. J. Chem. **94**, 1065 (2016).

[51] M. Piccardo, E. Penocchio, C. Puzzarini, M. Biczysko and V. Barone, J. Phys. Chem. A **119**, 2058 (2015).

[52] J.F. Stanton, J. Gauss and O. Christiansen, J. Chem. Phys. **114**, 2993 (2001).

[53] Z. Kisiel, J. Mol. Spectrosc. **218**, 58 (2003).

[54] Competition Science Vision, page 1635, February 2001.

[55] F. Mata, M.C. Martin and G.O. Sørensen, J. Mol. Struct. **48**, 157, (1978).

[56] B. Bak, D. Christensen, L. Hansen-Nygaard and J. Rastrup-Andersen, J. Mol. Spectrosc. **7**, 58 (1961).

[57] V. Van, J. Bruckhuisen, W. Stahl, V. Ilyushin and H.V.L. Nguyen, J. Mol. Spectrosc. **343**, 121 (2018).

[58] V. Van, W. Stahl and H.V.L. Nguyen, Phys. Chem. Chem. Phys. **17**, 32111 (2015).

[59] G.G. Brown, B.C. Dian, K.O. Douglass, S.M. Geyer, S.T. Shipman and B.H. Pate, Rev. Sci. Instrum. **79**, 053103 (2008).

[60] T. S. Little, J. Qiu and J. R. Durig, Spectrochim. Acta A **45**, 789 (1989).

[61] L. Nygaard, J.T. Nielsen, J. Kirchheiner, G. Maltesen. J.R. Andersen and G.O. Sørensen, J. Mol. Struct. **3**, 491 (1969).

[62] R.D. Nelson Jr., D.R. Lide and A.A. Maryott, Selected Values of electric dipole moments for molecules in the gas phase (NSRDS-NBS10), 1967.

[63] T. Ogata and K. Kozima, J. Mol. Spectrosc. **42**, 38 (1972).

[64] M.H. Sirvetz, J. Chem. Phys. **19**, 1609 (1951).

[65] P. Ramasami, Comput. Theor. Chem. **907**, 57 (2009).

[66] J. Kao and L. Radom, J. Am. Chem. Soc. **101**, 311 (1979).

[67] H. Ashish and P. Ramasami, Mol. Phys. **106**, 175 (2008).

[68] R. Hakiri, N. Derbel, H.V.L. Nguyen and H. Mouhib, Phys. Chem. Chem. Phys. **20**, 25577 (2018).

[69] V. Van, W. Stahl and H.V.L. Nguyen, ChemPhysChem **17**, 3223 (2016).

[70] U. Kretschmer, W. Stahl and H. Dreizler, Z. Naturforsch. **48a,** 733 (1993).

[71] U. Kretschmer and H. Dreizler, Z. Naturforsch. **48a,** 1219 (1993).

[72] J. Gripp, U. Kretschmer and H. Dreizler, Z. Naturforsch. **49 a,** 1059 (1994).

[73] U. Kretschmer, H. Hartwig and H. Dreizler, J. Mol. Spectrosc. **174,** 137 (1995).

[74] N. Hansen, H. Hartwig, U. Kretschmer and H. Mäder, Ber. Bunsenges. **100,** 1182 (1996).

[75] L. Pierce and M. Hayashi, J. Chem. Phys. **35**, 479 (1961).

[76] H. Dreizler, H.D. Rudolph and H. Schleser, Z. Naturforsch. **25a,** 1643 (1970).

[77] K. Okiye, C. Horise, D.G. Lister and J. Sheridan, Chem. Phys. Lett. **24,** 111 (1974).

[78] A.H. Saleck, M. Tanimoto, S.P. Belov, T. Klaus and G. Winnewisser, J. Mol. Spectrosc. **171,** 481 (1995).

[79] U. Kretschmer, Z. Naturforsch. **50a,** 666 (1995).

[80] R.D. Brown, P.G. Godfrey, D. McNaughton and K. Yamanouchi, Mol. Phys. **62,** 1429 (1987).